



## Microneedle-based electrodes with integrated through-silicon via for biopotential recording

Conor O'Mahony<sup>a,\*</sup>, Francesco Pini<sup>a,b</sup>, Alan Blake<sup>a</sup>, Carlo Webster<sup>a</sup>, Joe O'Brien<sup>a</sup>, Kevin G. McCarthy<sup>b</sup>

<sup>a</sup> Tyndall National Institute, University College Cork, Lee Maltings, Cork, Ireland

<sup>b</sup> Dept. Electrical and Electronic Engineering, University College Cork, Cork, Ireland

### ARTICLE INFO

#### Article history:

Received 16 September 2011

Received in revised form 26 April 2012

Accepted 27 April 2012

Available online 22 May 2012

#### Keywords:

Microneedle

Dry electrode

Potassium hydroxide

Electrocardiography (ECG)

Electromyography (EMG)

Biopotential

### ABSTRACT

The fabrication of a novel ultrasharp silicon microneedle array for use as a physiological signal monitoring electrode is described. This work uses double-sided silicon wafer patterning and anisotropic potassium hydroxide wet etching to simultaneously create a microneedle on the front side of the wafer, and a through-silicon via from the backside. Metal deposition on both the front and the back of the wafer then establishes electrical contact through this via between both sides of the electrode. This technique eliminates the limitations associated with other approaches that are used to create front-to-back electrical contact and that may be slow or cumbersome. Wearable electrode prototypes have been assembled using these arrays, and electrocardiography (ECG) and electromyography (EMG) recordings have been carried out to verify the functionality of the technique.

© 2012 Elsevier B.V. All rights reserved.

### 1. Introduction

Many organs in the human body, such as the heart, brain, muscles, and eyes, produce measurable electrical signals as a result of their activity. Electroencephalography (EEG), electrocardiography (ECG), and electromyography (EMG) are techniques used to record the electrical activity of the brain, heart and muscle, respectively. These output signals have typical bandwidths ranging from less than 1 Hz to 200 Hz and amplitudes vary from about 1  $\mu$ V to 10 mV, and can provide important diagnostic or clinical information; for example, EEG recordings may be used for seizure detection or brain-computer interfacing, ECG measurements can diagnose arrhythmias or heart failure, and EMG may be used to pinpoint neuromuscular disease or control prostheses [1].

These signals are sensed using electrodes placed at appropriate locations on the body. Conventional electrodes for measuring biopotentials are generally made of silver, silver-silver chloride or gold discs, and are connected to external instrumentation via a snap-on connector on the rear of the electrode. An electrolytic gel is often used to ensure a conductive interface between skin and electrode, and hence they are referred to as "wet electrodes". However, such wet electrodes are unsuited to long-term monitoring as the electrolytic gel tends to dry out over time, therefore leading

to higher skin contact impedance and a subsequent loss of signal quality during long-term measurements [2]. Skin abrasion is also often carried out prior to electrode placement in order to remove the resistive stratum corneum layer and improve skin-electrode contact. This procedure can cause problems with skin irritation and possible infection, and is uncomfortable for many patients [3]. So-called 'dry electrodes', which do not use electrolytic gel and are based on capacitive detection rather than electrochemical electrode-electrolyte interface, are therefore gaining popularity for long-term use [2,4,5], even though adequate and stable skin contact remains an issue.

#### 1.1. Microneedle-based electrodes for biopotential recording

Microneedles – sharp, micron-scale points made using micro-machining technologies from a wide variety of materials and originally intended for uses in transdermal drug and vaccine delivery [6] – have generated significant recent interest for use in long-term physiological signal monitoring. The outermost layer of the skin, the stratum corneum, is only 10–20  $\mu$ m thick but is largely composed of dead skin cells. It is therefore highly resistive and greatly degrades signal quality. Electrically conductive, microneedle-based 'dry electrodes' can be used to pierce this layer and make direct contact with the moist, highly conductive epidermal layers immediately underneath, thereby reducing the electrode-skin impedance and enhancing measurement accuracy whilst eliminating the need for skin abrasion and/or gel application

\* Corresponding author. Tel.: +353 21 4904200; fax: +353 21 4904058.  
E-mail address: [conor.omahony@tyndall.ie](mailto:conor.omahony@tyndall.ie) (C. O'Mahony).

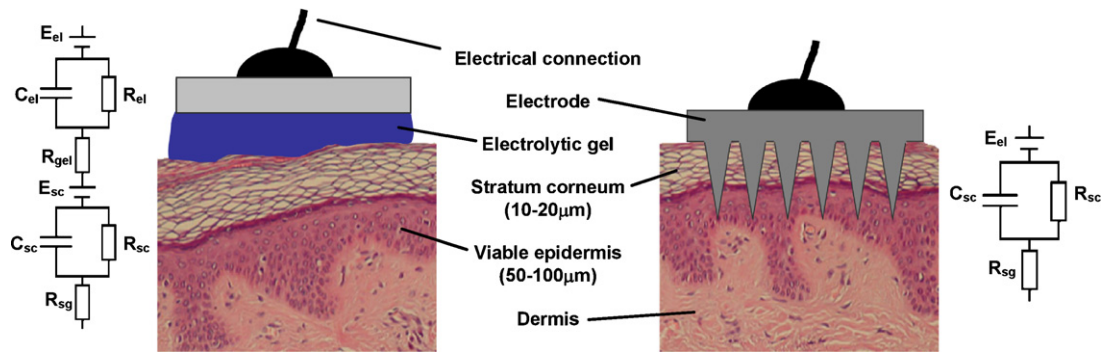


**Fig. 1.** Cross-sectional schematic and simplified electrical model of conventional wet (left) and microneedle-based dry electrodes (right). Microneedles eliminate the requirement for skin preparation and the use of electrolytic gels by making direct contact with the conductive, underlying skin layers [10].

prior to electrode attachment [7–9]. Furthermore, microneedle lengths can be such that they do not stimulate nerve endings within the skin, and so the use of these electrodes is painless.

A simplified electrical model of both microneedle-based and standard wet electrodes [10] is shown in Fig. 1.

The basic wet electrode may be modelled as an RC component in series with a resistive gel. The untreated stratum corneum layer also has both a resistive and a capacitive component and the underlying viable epidermal layers are assumed to be purely resistive. Half-cell potentials are generally present due to the different ionic concentrations across the gel–stratum corneum and electrode–gel interfaces. Use of a dry, microneedle-based electrode eliminates the gel component, bypasses the stratum corneum and allows the electrode to make direct contact with the resistive epidermal layers. It is clear that use of a microneedle-based electrode greatly simplifies the electrode–skin interface.

### 1.2. Electrical connection to microneedle-based dry electrodes

Several examples of silicon microneedle-based dry electrodes have already been demonstrated. However, in order not to interfere with the skin–electrode interface, the electrical connection to the outside world must be placed on the back of the electrode. This requirement means that electrical contact must be established between the front and rear surfaces of the electrode, a process that has previously been done by making contacts on individual microneedle die after wafer singulation [11,12,18], but this is time consuming and unsuited to volume production. Alternatively, a through-silicon via (TSV) can be made and metal-coated at wafer level after the microneedles are formed [13,14], although this adds cost by requiring extra time and processing steps. Since recording electrodes are cheap and disposable devices, there is therefore a need for a microneedle-based dry electrode that is fabricated using a process suited for rapid, economical, high-volume manufacture.

Using wet etching techniques, we have previously fabricated 50–800  $\mu\text{m}$  tall ultrasharp silicon microneedles for a range of biomedical applications [15]. This work describes the extension of that potassium hydroxide-based anisotropic etch process to create viable electrode arrays using just a single silicon etch step. Double-sided wafer patterning and a detailed knowledge of the anisotropic etch process is used to simultaneously create a microneedle on the front side of the wafer, and a through-silicon via from the backside. Metal deposition on both the front and the back of the wafer then establishes electrical contact through this via between both sides of the electrode. This rapid, wafer-level, single-etch process eliminates the need for additional processing in order to establish front-to-back electrical contact.

Wearable electrode prototypes have been assembled using these arrays, and preliminary electrocardiography (ECG) and

electromyography (EMG) recordings have been carried out to verify the functionality of the manufacturing process.

## 2. Electrode fabrication

### 2.1. Microneedle design and fabrication

The microneedle electrodes were fabricated at the Tyndall National Institute using potassium hydroxide (KOH) wet-etching techniques. The microneedle design, mask dimensions and the theory behind the etch mechanism has been extensively described in [15,16], and a schematic of the electrode fabrication process is depicted in Fig. 2. The starting material is a 525  $\mu\text{m}$  thick, boron doped, 100 mm diameter monocrystalline silicon wafer, orientated in the  $\langle 100 \rangle$  direction and into which marks denoting the precise crystal alignment are etched. A hard masking layer of 350  $\text{\AA}$  silicon oxide/1000  $\text{\AA}$  silicon nitride is then deposited and patterned in square masks using standard photolithography techniques; the dimensions of these square masks determine the array pitch and needle geometry. The mask pattern was etched into the nitride layer using a plasma etch process and the remaining resist stripped.

To generate a through-silicon via (TSV), square openings, the sides of which were aligned to the  $\langle 110 \rangle$  crystal axis were patterned on the rear of the wafer using a lithography process identical to that outlined above. It is well known that KOH etching of such openings produces inverted four-sided pits defined by the  $\langle 111 \rangle$  crystal planes, which have an angle of  $54.74^\circ$  to the horizontal [17]. The depth of such a pit,  $d$ , is related to the mask opening side length  $l$  by  $l = 2d/\tan(54.74^\circ)$ .

The oxide layers were then removed from the open areas using hydrofluoric acid (HF), and the wafer was etched using a hot aqueous KOH solution. Needle formation is based on the anisotropic etch behaviour of monocrystalline silicon in KOH, a property of the crystal structure that causes each group of crystal planes to etch at a different rate. The sides of the square nitride mask are aligned to the particularly slow-etching  $\langle h11 \rangle$  plane; the faster-etching  $\langle h12 \rangle$  planes are exposed to the KOH at the convex corners of the square. As two of these fast-etching planes are etched from each corner, an octagonal needle shape is generated when the eight planes meet. After a front etch depth  $t$ , the final needle has a height  $h$ , is comprised of eight  $\langle 263 \rangle$  planes, a base of  $\langle 212 \rangle$  planes and it has a height:base diameter aspect ratio of 3:2.

A pyramidal is simultaneously formed from the backside of the wafer, which intersects with the front side to form a TSV if the two conditions: (i)  $t + d >$  substrate thickness and (ii)  $t > d$  are satisfied. In this particular case, the initial substrate thickness is 525  $\mu\text{m}$  thick and the front etch depth is approximately 330  $\mu\text{m}$ ; a rear pit of greater than 195  $\mu\text{m}$  in depth is therefore required to achieve an intersection with the front surface.

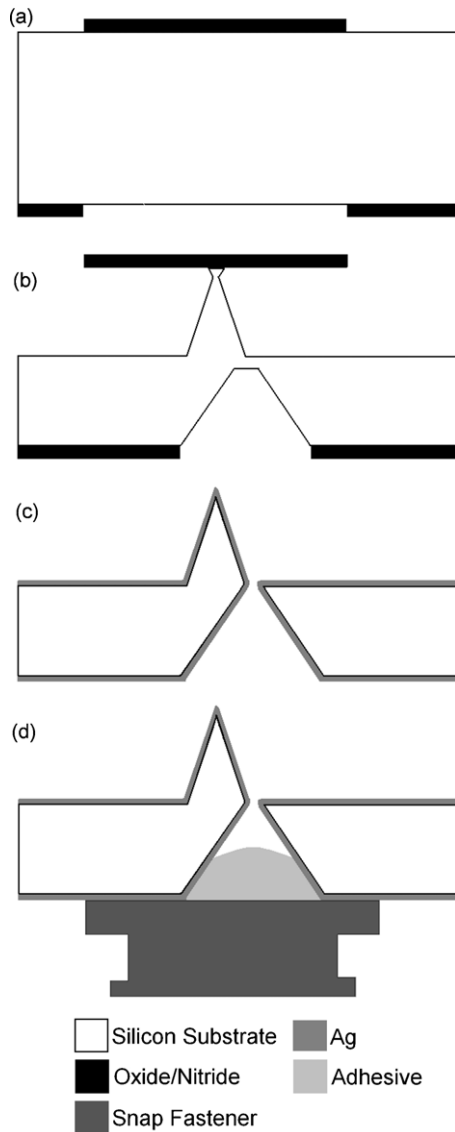


**Fig. 2.** Microneedle fabrication: (a) front and rear mask definition; (b) intermediate stage of device formation, illustrating the formation of microneedle and rear pit; (c) double-sided silver evaporation after completion of etch, (d) prototype device assembly depicting snap fastener glued to rear of electrode.

Note that the TSV must be carefully designed: a shallow pit will not intersect with the front side of the wafer at all, but a deep pit will break through before microneedle etching is complete, and expose the fast-etching  $\langle 100 \rangle$  planes at the intersection to the etchant for the remainder of the etching time. This results in rapid and undesirable widening of the intersection if  $d \gg t$ .

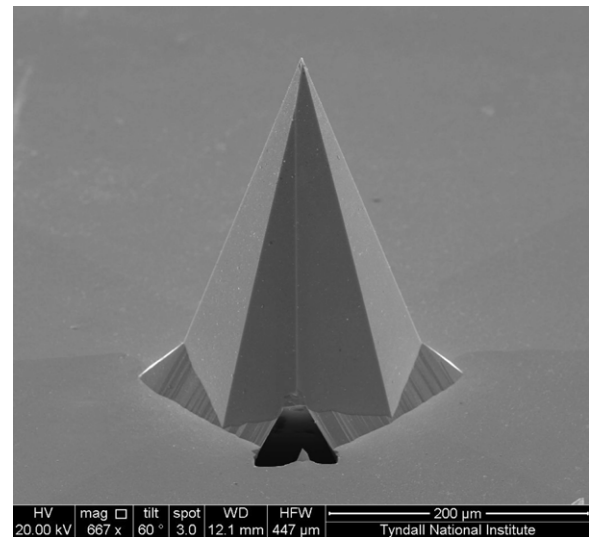
A scanning electron microscopy image of a final needle is shown in Fig. 3. The TSV is clearly visible at the base of the microneedle.

Fig. 4 illustrates the pyramidal pit and opening from the rear of the microneedle.

The etch process was also simulated using the VisualTAPAS wet etch simulator [19], and the output is shown in Fig. 5. The simulated shape and position of the TSV agrees well with experimental results.

## 2.2. Electrode assembly

The arrays used in this study consisted of a  $5 \times 5$  arrangement of  $300 \mu\text{m}$  tall needles located at a pitch of  $1.2 \text{ mm}$  on a  $7 \text{ mm} \times 7 \text{ mm}$  die, Fig. 6.



**Fig. 3.** Scanning microscopy image of a silicon microneedle and through-silicon via opening. This needle is  $283 \mu\text{m}$  tall.

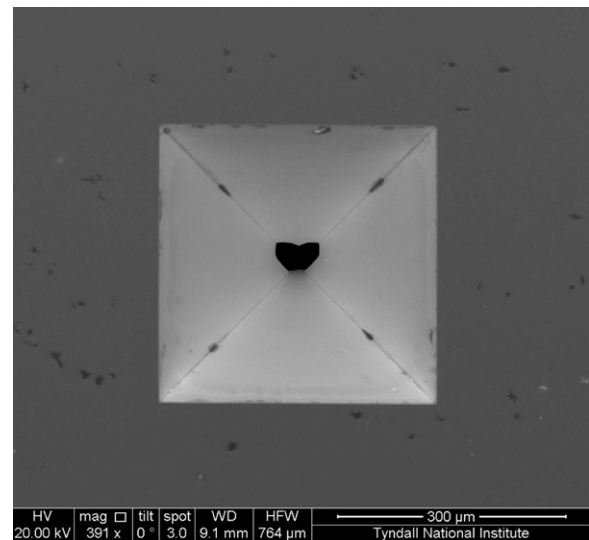


**Fig. 4.** Plan view of four-sided pit at the rear of the wafer. The black area which constitutes the front-to-back surface intersection is at the centre (bottom) of the pit.

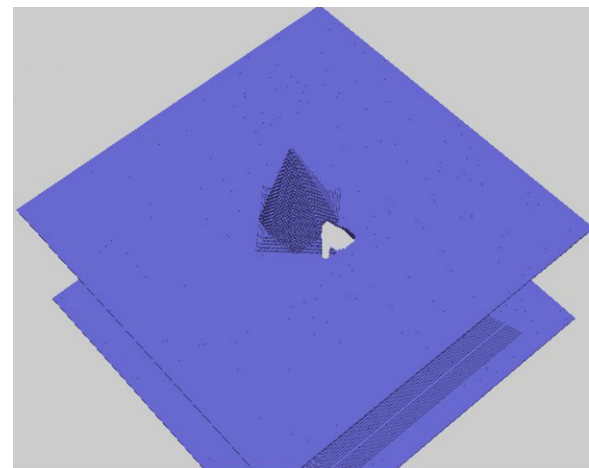


**Fig. 5.** Simulated representation of the front surface of the wafer, showing the microneedle and TSV, from the VisualTAPAS simulator. The simulation agrees well with the results shown in Fig. 3.

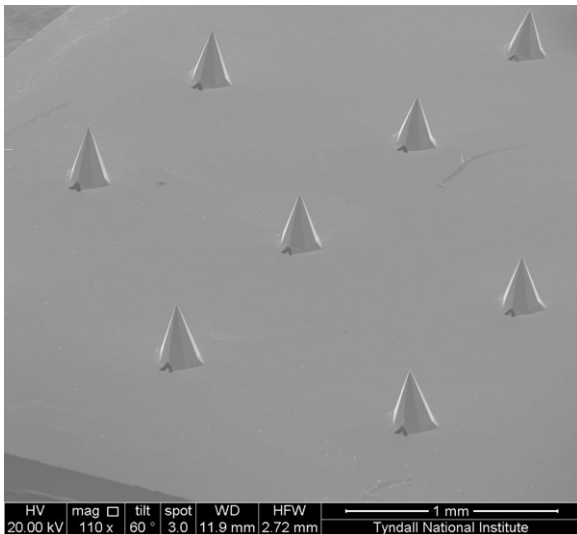


**Fig. 6.** Front surface of microneedle-based dry electrode, illustrating an array of microneedles. A through-silicon via contact is visible at the base of each microneedle.

A 10 nm thick layer of titanium was thermally evaporated onto both sides of the wafer to act as an adhesion layer. A 200 nm thick Ag layer was then deposited, also using thermal evaporation, and the wafer was diced into individual electrode arrays. Future designs will be also chlorided using an electrochemical process to produce an Ag/AgCl layer in order to generate a stable, low-noise skin interface. In order to verify that silver had successfully been deposited onto the sidewalls of the through-silicon via and that front-to-back electrical contact was achieved at the intersection of the TSV and front surface of the die, contact measurements between the front (microneedle side) of the die and rear (TSV side) of the die were carried out using a handheld multimeter. This contact is resistive in nature with a resistance of approximately  $(0.7 \pm 0.2)$  Ohms. It should be noted that we have designed 25 TSVs on each electrode (one per needle). This reduces the electrode front-to-back resistance and increases the yield of the TSV coating process.

In order to create a wearable prototype and facilitate preliminary tests, the electrodes were interfaced to a standard electrode (2239 Red Dot Monitoring Electrode, 3M Healthcare, Germany), from which the electrolytic gel was removed, using a conductive adhesive (186-3616, Radionics, Ireland), Fig. 7. This solution provides both an adhesive backing and a metal snap fastener for interface with recording equipment.

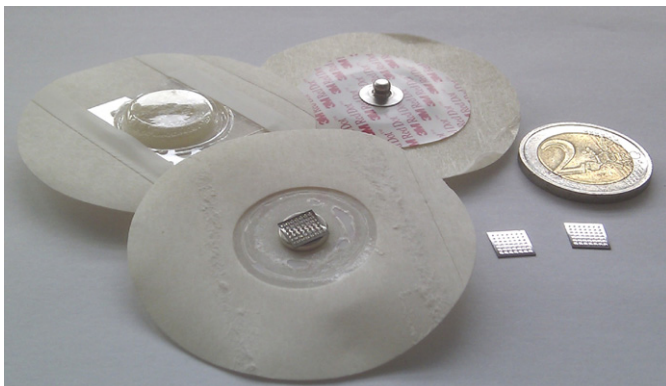


**Fig. 7.** Microneedle arrays and assembled prototype electrodes. A traditional wet electrode is shown on the rear left of the image.

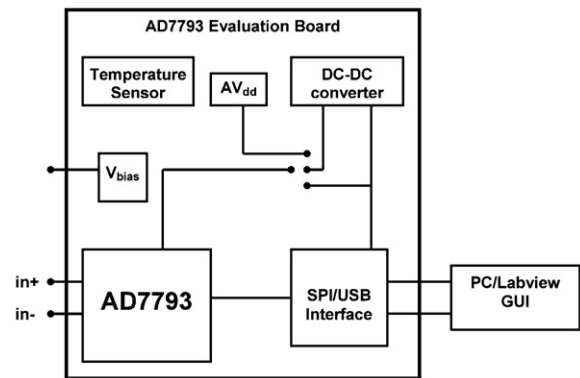
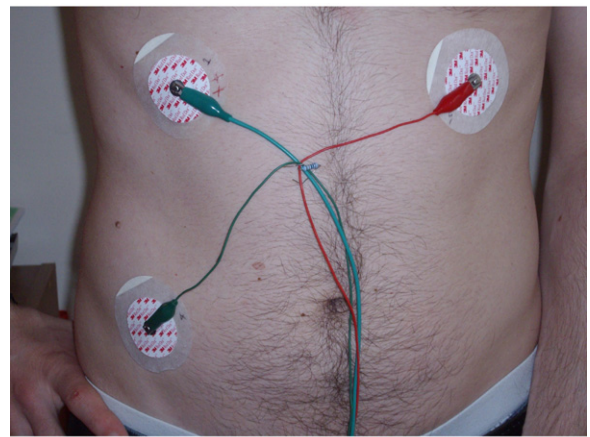


**Fig. 8.** Top: block diagram of the recording circuitry. Bottom: physical placement of the electrodes for ECG measurement.

### 3. Biopotential recording

#### 3.1. Experimental methodology and setup

In order to record biopotential signals, an evaluation board (AD7793 Evaluation Board, Analog Devices), containing the AD7793 chip (3-channel, low-noise, low-power, 24 bit  $\Sigma$ - $\Delta$  ADC with on chip differential amplifiers and reference) has been used. The board is interfaced to a PC using a USB cable and a LabView GUI is used to visualize the recorded inputs.

Physiological signal recordings were performed on a 27-year-old Caucasian male subject who gave informed consent. Measurements were performed using a three-electrode arrangement of standard Ag/AgCl wet electrodes (14222, Red Dot Monitoring Electrode, 3M Healthcare, Germany), and were then repeated using the same arrangement of dry microneedle electrodes. In both cases the electrodes were applied to the same body location and without prior skin preparation.

The signal was read differentially through two electrodes located on the chest of the subject whilst a bias voltage was applied to the body through a third electrode located on the lower right torso of the subject. The bias voltage was chosen to be half way between the supply voltage and the ground of the evaluation board ( $V_{BIAS} = 1.65$  V). The electrode setup for ECG measurement is shown in Fig. 8.

The same three-electrode setup is used to measure the EMG biopotential of the tricep. Two recording electrodes were placed on the tricep of the right arm of the subject and one reference electrode placed near the internal part of the elbow, where the electrical activity of the human body is negligible. The test was repeated using both microneedle-based electrodes and standard 'wet'

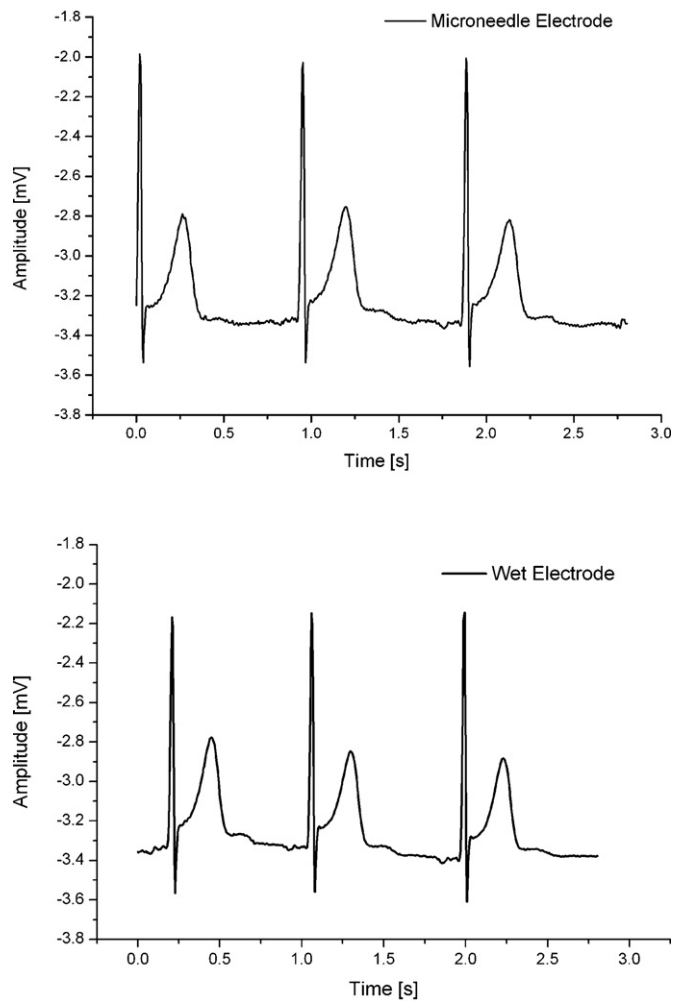


**Fig. 9.** Electrocardiographs obtained using (top) a set of microneedle-based dry electrodes and (bottom) pre-gelled wet electrodes (Type 14222, Red Dot Monitoring Electrode, 3M Healthcare, Germany).

electrodes. As with the ECG measurements, the reference electrode was supplied with a DC voltage that was half the supply voltage of the electronic board and the two recording electrodes were reading the EMG signal differentially.

### 3.2. Electrocardiograph recording

Fig. 9 illustrates a comparison between electrocardiographs obtained using standard wet electrodes and the dry microneedle-based electrodes described in this work. The microneedle measurements are very similar to those recorded using conventional wet electrodes. The typical cardiac signatures of the QRS-complex and T-wave are clearly visible; the heart rate in this case is 67 beats per minute. Rejection of 50 Hz interference is highly effective because the recording electronics (both AD7793 evaluation board and PC) is battery supplied and the leads connecting the electrodes to the acquisition board are carefully twisted, in order to reduce electromagnetic coupling. The behaviour of both traces in the interval between two different heartbeats shows similar noise performances for the two types of electrodes.

This preliminary work proves the ability of dry microneedle-based electrodes manufactured using this process to adequately sense and record cardiac signals and to measure heart rates.

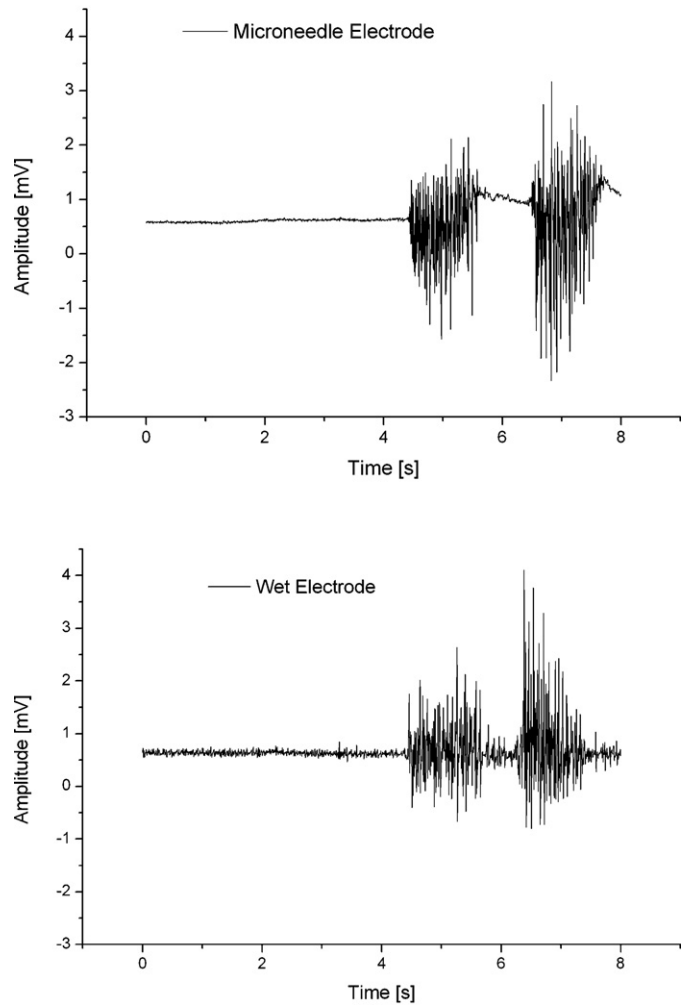


**Fig. 10.** Electromyograms obtained from the bicep muscle using (top) a set of microneedle-based dry electrodes and (bottom) pre-gelled wet electrodes (Type 14222, Red Dot Monitoring Electrode, 3M Healthcare, Germany).

### 3.3. Electromyogram recording

After a period of relaxation, the tricep muscle was contracted for two short periods and the recorded EMG signals, shown in Fig. 10, clearly reflect the contractions of the muscle. The amplitude of the EMG recorded during contraction of the muscle using either wet or dry electrodes is very similar. This measurement again demonstrates the ability of dry microneedles electrodes to sense and record surface biopotential EMG signals with good fidelity. Similar results have been obtained from the bicep muscle (data not shown).

## 4. Discussion

This work has reported on the development of a viable manufacturing process for microneedle-based electrodes. Although this work has clearly shown that electrodes fabricated using this procedure are capable of measuring biopotential signals when used in the same manner as conventional 'wet' electrodes, there are several barriers to market acceptance of such devices, including a perception that infection may occur as the outer skin layers are pierced and that these micron-scale structures may appear to be relatively fragile.

We consider the issue of infection (either due to microbial transport or microneedle breakage) after microneedle application

unlikely. Using silicon microneedles identical to these, it has previously been concluded that microneedle puncture resulted in significantly less microbial penetration than did hypodermic needle puncture, and that application of microneedle arrays to skin in an appropriate manner should not cause either local or systemic infection in normal circumstances in immune-competent patients [20]. It has also been shown that the pores created in skin as a result of microneedle application close on a timescale of the order of hours [21,22]. These superficial microchannels heal significantly faster than wounds caused by hypodermic syringe use, and this rapid closure should further reduce the risk of infection.

It has also been shown that use of these needles is painless, although a sensation of pressure due microneedle application may be noted [22]. We have previously demonstrated that 280  $\mu\text{m}$  tall needles penetrate approximately 180  $\mu\text{m}$  into the skin [21], bypassing the stratum corneum and entering the epidermis, although the dermal–epidermal junction is not reached due to tissue compression and deformation. This penetration depth is not sufficient to stimulate the underlying nerve endings enough to cause a perception of pain by the subject. No pain or skin irritation has been reported during the experiments reported in this work.

Although occasional failure of silicon-based dry electrodes based on cylindrical microneedles has been reported [13], we have not seen fracture of these devices when used under normal conditions. As this particular type of needle is conical, the structure has a very high area moment of inertia and so the risk of failure due to buckling is low [23]. Furthermore, the needle–skin interfacial area increases with insertion depth. This interaction reduces the pressure on the weak silicon planes and lessens the likelihood of failure. In addition, the elastic nature of the skin and the force exerted by the skin on the sloped sidewalls of the needle results in an upward component of force that would push a broken needle out of the skin. In addition, the epidermal skin layers are renewed in such a manner that the outer skin cells are pushed upwards and shed from the body every 2–3 weeks [24], which assists in ejecting foreign particles from the skin.

In order to assess microneedle reliability during skin insertion when arrayed in this particular configuration, electrodes were applied to the ventral forearm using moderate finger pressure and held in position using a swaying motion for approximately 10 s. Following removal, 100 randomly selected microneedles were inspected using an optical microscope (SZX12, Olympus Microscopy, UK). No fracture or failure of any needle was identified. In a majority of cases, the silver coating appears to have been partially removed from the tip region of the microneedle as shown in Fig. 11 (bottom). Although this should not pose a medical risk due to the antimicrobial and biocompatible nature of silver [25], the minimally invasive nature of the microneedles and the extremely small quantities of silver involved, estimated at  $(2\text{--}20) \times 10^{-12}$  kg per needle, it is nevertheless undesirable and could lead to problems with the long-term stability of the electrodes. Further work will improve coating reliability by using modified adhesion layers and techniques such as atomic layer deposition.

It is also interesting to note that both CE (European Conformity) and FDA (Food and Drug Administration) 510k approval has already been granted for microneedle-based devices for transdermal delivery applications [26,27]. This indicates the growing acceptance of silicon-based, minimally invasive microneedle technologies by regulatory bodies.

Although these initial results are promising, future device development is required. This includes a detailed analysis of the influence of electrode design (e.g. microneedle height, needle and via density, coating metal type and thickness) on electrical and biomechanical performance. Future work will also gather additional biopotential

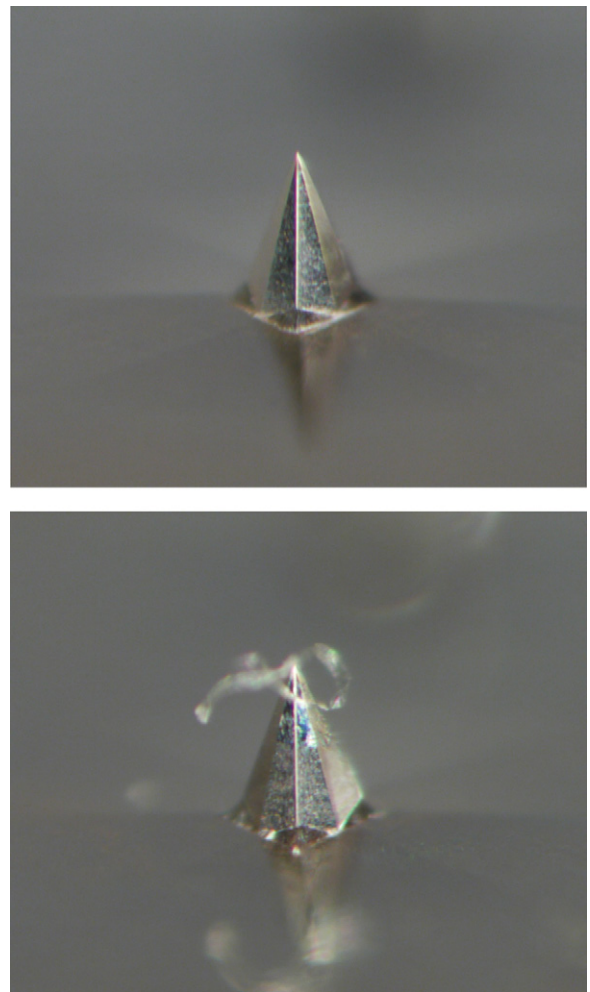


**Fig. 11.** Microneedle before (top) and after (bottom) skin insertion using moderate finger pressure. Although some skin material is usually visible on the surface of the microneedles and silver appears to have been partially removed from microneedle tips, no structural damage is visible either to the tips or to the body of the needles.

data and assess the stability and performance of these devices in static, dynamic and long term monitoring applications.

## 5. Conclusions

This paper has demonstrated the design, fabrication and preliminary application of a novel, microneedle-based dry electrode for biopotential monitoring. A double-sided KOH bulk etch technique has been used to simultaneously fabricate an ultrasharp microneedle array on the front side of a wafer, and a through-silicon via from the backside. This device may be subsequently coated with metal to establish front-to-back electrical contact at wafer level, thereby eliminating the limitations associated with other manufacturing techniques.

Initial electrocardiography (ECG) and electromyography (EMG) measurements show good results in terms of signal acquisition and fidelity, and prove the ability of dry microneedle electrodes to accurately sense physiological signals. The output signals are comparable with those obtained using standard wet electrodes, but dry electrodes require no skin abrasion and do not suffer from the problem of gel dehydration. They are therefore promising for use in long-term monitoring applications.

## Acknowledgements

The authors would like to thank the Tyndall Institute's Central Fabrication Facility for device processing. This work was partially supported by Enterprise Ireland under the Commercialisation Fund programme, and by Science Foundation Ireland through the 'Efficient Embedded Digital Signal Processing for Mobile Digital Health' Strategic Research Cluster.

## References

- [1] N.V. Thakor, Biopotentials and electrophysiology measurement, in: J.G. Webster (Ed.), *The Measurement, Instrumentation and Sensors Handbook*, CRC Press, Boca Raton, 1998 (Chapter 74).
- [2] A. Searle, L. Kirkup, A direct comparison of wet, dry and insulating bioelectric recording electrodes, *Physiological Measurement* 21 (2001) 271–283.
- [3] H.W. Tam, J.G. Webster, Minimizing electrode motion artifact by skin abrasion, *IEEE Transactions on Biomedical Engineering* 24 (2) (1977) 134–139.
- [4] C.-L. Chang, C.-W. Chang, H.-Y. Huang, C.-M. Hsu, C.-H. Huang, J.-C. Chiou, C.-H. Luo, A power-efficient bio-potential acquisition device with DS-MDE sensors for long-term healthcare monitoring applications, *Sensors* 10 (2010) 4777–4793.
- [5] B.A. Taheri, R.T. Knight, R.L. Smith, A dry electrode for EEG recording, *Electroencephalography and Clinical Neurophysiology* 90 (1994) 376–383.
- [6] S. Coulman, C. Allender, J. Birchall, Microneedles and other physical methods for overcoming the stratum corneum barrier for cutaneous gene therapy, *Critical Reviews in Therapeutic Drug Carrier Systems* 23 (2006) 205–258.
- [7] L.M. Yu, F. Tay, D.G. Guo, L. Xu, M.N. Nyan, F.W. Chong, et al., A MEMS-based bioelectrode for ECG measurement, in: *Proc. IEEE Sensors*, Lecce, Italy, 26–29 October 2008, pp. 1068–1071.
- [8] R. Lutttge, S.N. Bystrova, M.J.A.M. van Putten, Microneedle array electrode for human EEG recording, *Proceedings of International Federation for Medical and Biological Engineering* 22 (10) (2009) 1246–1249.
- [9] P. Griss, H.K. Tolvanen-Laakso, P. Meriläinen, G. Stemme, Micromachined electrodes for biopotential measurements, *IEEE Transactions on Biomedical Engineering* 49 (6) (2002) 597–604.
- [10] J.G. Webster, *Medical Instrumentation: Application and Design*, 4th ed., Wiley, New Jersey, 2010.
- [11] Y. Wang, K. Guo, W.-H. Pei, Q. Gui, X.-Q. Li, H.-D. Chen, et al., Fabrication of dry electrode for recording bio-potentials, *Chinese Physics Letters* 28 (1) (2011) 010701.
- [12] D.G. Guo, F.E.H. Tay, L.M. Yu, L. Xu, M.N. Nyan, F.W. Chong, et al., A wearable BSN-based ECG-recording system using micromachined electrode for continuous arrhythmia monitoring, in: *Proc. 5th International Workshop on Wearable and Implantable Body Sensor Networks*, Hong Kong, China, 1–3 June 2008, pp. 41–44.
- [13] P. Griss, P. Enoksson, H.K. Tolvanen-Laakso, P. Meriläinen, S. Ollmar, G. Stemme, Micromachined electrodes for biopotential measurements, *Journal of Microelectronic Systems* 10 (1) (2001) 10–16.
- [14] S.-O. Choi, Y.-C. Kim, J.-H. Park, J. Hutcheson, H.S. Gill, Y.-K. Yoon, M.R. Prausnitz, M.G. Allen, An electrically active microneedle array for electroporation, *Biomedical Microdevices* 12 (2010) 263–273.
- [15] N. Wilke, M.L. Reed, A. Morrissey, The evolution from convex corner undercut towards microneedle formation: theory and experimental verification, *Journal of Micromechanics and Microengineering* 16 (2006) 808–814.
- [16] N. Wilke, A. Morrissey, Silicon microneedle formation using modified mask designs based on convex corner undercut, *Journal of Micromechanics and Microengineering* 17 (2007) 238–244.
- [17] M.J. Madou, *Fundamental of Microfabrication*, 2nd ed., CRC Press, Boca Raton, 2001.
- [18] S. Rajaraman, J.A. Bragg, J.D. Ross, M.G. Allen, Micromachined three-dimensional electrode arrays for transcutaneous nerve tracking, *Journal of Micromechanics and Microengineering* 21 (2011) 085014.
- [19] M.A. Gosalvez, Y. Xing, K. Sato, R.M. Nieminen, Atomistic methods for the simulation of evolving surfaces, *Journal of Micromechanics and Microengineering* 18 (2008) 055029.
- [20] R.F. Donnelly, T.R. Singh, M.M. Tunney, D.I. Morrow, P.A. McCarron, C. O'Mahony, A.D. Woolfson, Microneedle arrays allow lower microbial penetration than hypodermic needles in vitro, *Pharmaceutical Research* 26 (11) (2009) 2513–2522.
- [21] J. Enfield, M.-L. O'Connell, K. Lawlor, E. Jonathan, C. O'Mahony, M. Leahy, In vivo dynamic characterization of microneedle skin penetration using optical coherence tomography (OCT), *Journal of Biomedical Optics* 15 (4) (2010) 046001–46007.
- [22] M.I. Haq, E. Smith, D.N. John, M. Kalavala, C. Edwards, A. Anstey, A. Morrissey, J.C. Birchall, Clinical administration of microneedles: skin puncture, pain and sensation, *Biomedical Microdevices* 11 (1) (2009) 35–47.
- [23] W.G. Smith, Analytic solutions for tapered column buckling, *Computers and Structures* 28 (5) (1988) 677–681.
- [24] J.A. Cowen, R.E. Imhof, P. Xiao, Opto-thermal measurement of stratum corneum renewal time, *Analytical Sciences* 17 (2001) 353–356.
- [25] L.C. Fung, A.E. Khoury, S.I. Vas, C. Smith, D.G. Oreopoulos, M.W. Mittelman, Biocompatibility of silver-coated peritoneal dialysis catheter in a porcine model, *Peritoneal Dialysis International* 16 (1996) 398–405.
- [26] CE Certificate of Conformity 2120317CN, [www.nanopass.com/upfiles/A/2120317ce01%20\(4\).pdf](http://www.nanopass.com/upfiles/A/2120317ce01%20(4).pdf) (retrieved 07.02.12).
- [27] FDA 510k Summary K092746, [www.accessdata.fda.gov/cdrh\\_docs/pdf9/K092746.pdf](http://www.accessdata.fda.gov/cdrh_docs/pdf9/K092746.pdf) (retrieved 07.02.12).

## Biographies

**Conor O'Mahony** received the B.Sc. (Physics) degree from University College Cork in 1998, and the M.Eng.Sc. and Ph.D. degrees in 2000 and 2004, respectively, for work on radio-frequency micromachined switches carried out at the National Microelectronics Research Centre, Cork, Ireland. From 2004 to 2007 he was a Staff Researcher at the Tyndall National Institute, with interests in microfabrication technologies spanning the fields of radio-frequency MEMS switches and varactors, environmental sensors, wafer-level packaging and modelling of MEMS. In 2008 he assumed responsibility for the management of Tyndall's microneedle research programme, which fabricates silicon microneedle-based devices for a wide range of biomedical applications including drug and vaccine delivery, electroporation and physiological signal monitoring. He has published over one hundred research papers in journals and at conferences, and has filed eight patent applications in the field of MEMS and micromachining, several of which have been licensed to industrial collaborators. He is currently Chair of the 2nd International Conference on Microneedles (Microneedles 2012).

**Francesco Pini** received the B.Sc. and M.Sc. degrees in electrical and electronic engineering from Politecnico di Milano, Milan, Italy, in 2005 and 2008, respectively. Since 2009 he is working towards his Ph.D. at the Tyndall National Institute, University College Cork, Ireland and in September 2011 he joined Silicon and Software Systems (S3 Group), Cork, Ireland, as an analog/RFIC design engineer. His main research interests are in biosensor development and characterization, novel on-chip architectures and integrated circuit design for biomedical applications.

**Alan Blake** received the B.Sc. in Applied Physics from the University of Limerick, Ireland, in 1997. In 2000, he joined the Silicon Fabrication Laboratory at the Tyndall National Institute, Cork, Ireland, as a Process Engineer. His current research interests lie in the fields of MEMS, nanofabrication and post-CMOS device processing.

**Carlo Webster** is a Business Development Executive with the Tyndall National Institute, Cork, Ireland.

**Joe O'Brien** received the B.Sc. (Chemistry) in 1985 from University College Cork, and is currently a Senior Process Fabrication Engineer with the Tyndall Microsystems Fabrication Group. His career at NMRC/Tyndall has involved working in all aspects of lithography from Broadband to Deep UV to Electron Beam Lithography. Over the years he has been involved in a number of projects including Electron Beam resist characterization for Hybrid Bipolar transistors (ESA), the development of novel submicron Schottky Barrier diodes and Beam Lead diode technology for the European Space Agency (ESA). He is currently working on Advanced Lithographic projects focusing on High Aspect Ratio photo resist fabrication routes for micromachining together with Advanced Silicon Etching incorporating ASE-BOSCH process and Advanced Oxide Etching (AOE) in the Microsystems Fabrication group. He also heads the Microsystems Wafer bonding facility.

**Kevin McCarthy** obtained the B.E., M.Eng.Sc. and Ph.D. degrees from University College Cork (UCC) in 1982, 1986 and 1992 respectively. He joined the Department of Electrical and Electronic Engineering, UCC, in October 2000 where his primary research interests are in microelectronic devices and circuits for RF and mixed-signal applications. Previously, he was a senior research scientist at the National Microelectronics Research Centre, Cork (NMRC, 1993–2000) where he was involved in the simulation of advanced MOSFET and bipolar devices for digital and analogue applications, especially the development and evaluation of accurate device models for circuit simulation and statistical analysis in support of yield enhancement strategies such as Design for Manufacturability (DFM). Before joining NMRC/UCC he worked with Analog Devices, Limerick (1982–1984, 1990–1993) in product engineering and CAD engineering roles. Kevin is a member of the technical program committee of the IEEE International Conference on Microelectronic Test Structures (ICMTS) and has also served on the technical program committees of the IEEE International Symposium on Radio Frequency Integrated Circuits (RFIC) and the European Solid-State Device Research Conference (ESSDERC).